Nonlithographic nanowire-array tunnel device: Fabrication, zero-bias anomalies, and Coulomb blockade

D. N. Davydov
Department of Chemistry, University of Toronto, 80 St. George Street, Toronto, Ontario, Canada M5S 3H6

J. Haruyama
Department of Electrical and Computer Engineering, University of Toronto, 10 King's College Road, Toronto, Ontario, Canada M5S 1A4

D. Routkevitch
Department of Chemistry, University of Toronto, 80 St. George Street, Toronto, Ontario, Canada M5S 3H6

B. W. Statt
Department of Physics, University of Toronto, Toronto, Ontario, Canada M5S 1A7

D. Ellis
Department of Electrical and Computer Engineering, University of Toronto, 10 King's College Road, Toronto, Ontario, Canada M5S 1A4

M. Moskovits
Department of Chemistry, University of Toronto, 80 St. George Street, Toronto, Ontario, Canada M5S 3H6 and Photonics Research Ontario, 10 King's College Road, Toronto, Ontario, Canada M5S 1A4

J. M. Xu
Department of Electrical and Computer Engineering, University of Toronto, and Photonics Research Ontario, 10 King's College Road, Toronto, Ontario, Canada M5S 1A4

(Received 1 December 1997)

Coulomb blockade (CB) was observed in Al/aluminum oxide/Ni nanowire single-junction arrays fabricated by electrochemical deposition of Ni into porous aluminum oxide nanotemplates. The bias dependence of the tunneling current and the temperature dependence of the zero-bias anomalies observed in the tunneling spectra are shown to accord well with the theory of Nazarov for CB in systems where the leads play a significant role. Direct scanning tunneling microscopy measurements of the nanowire leads resistance confirms it to be the regime required by the theory. [S0163-1829(98)02521-1]

A great deal of brilliant science and engineering involving mesoscopic structures was made possible over the past decade through the use of advanced lithographic technologies. These techniques seem to be approaching their economical if not their technological limits for fabricating one-dimensional (1D) and 0D nanostructures of very small size, thereby creating an opportunity for introducing alternative approaches to nanostructure fabrication through such means as selective deposition into templates.[1–3] An attractive template candidate is anodic aluminum oxide (AAO) which self-organizes into a hexagonal array of uniform nanopores[4] with pore densities up to 10^{12} cm^{-2} and pore diameters down to 4 nm. A variety of nanostructures can be created using AAO templates by depositing metals, semiconductors, organics, or their combinations into the pores.

The tunneling probability through single tunnel junctions of small enough capacitance and at low enough temperatures such that $kT < e^2/2C$, is strongly suppressed Coulombically. The quantum-mechanical theory of this effect, referred to as Coulomb blockade (CB), was reported by Averin and Likharev[5] for a single junction. Additionally, a number of successful Coulomb blockade studies performed on multiple junctions of metal clusters[6,7] or nanolithographic structures[8,9] have been reported. In contrast, few reports exist demonstrating clear CB in single junction systems[8,10,9] because in single junctions the effect is easily masked by the effect of the external leads unless a high enough lead resistance such that $R_L >> R_Q = h/2e^2$ is directly connected to the single junction.[9,11] In practice, it is very difficult to achieve this condition in single junctions while retaining a small stray capacitance $< 10^{-16}$ F. In a number of studies, the high lead resistance was achieved by connecting a few tunnel junctions in series.[8,12]

In this paper we report observation of CB in electrochemically fabricated arrays of single tunnel junctions formed at the tips of parallel Ni nanowires. The nickel in the nanowires is disordered and, hence, the nanowire resistance is found to be sufficiently high to overcome the aforementioned effect of low lead resistance. Additionaly, the stray capacitance was found to be very small [$\sim(3-8)\times10^{-17}$ F]

 © 1998 The American Physical Society

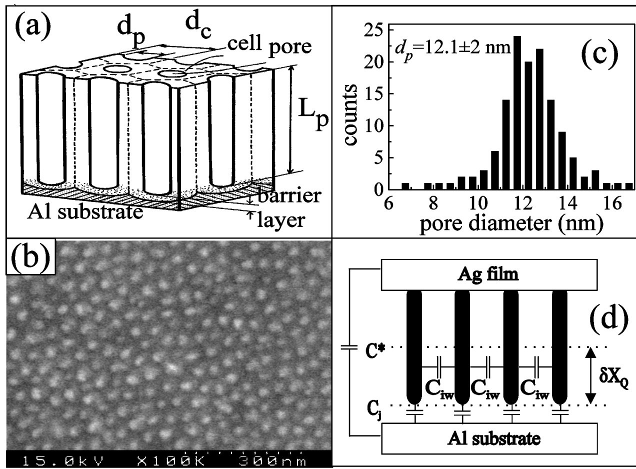

FIG. 1. (a) Schematic cross-sectional view of an AAO template, (b) Top-view SEM micrograph of Ni nanowire array, (c) nanowire diameter distribution, (d) schematic of device indicating sources of stray capacitance.

in our structures. The simple technology described is potentially applicable to device fabrication.

A schematic cross-sectional view of the structure of the AAO template is shown in Fig. 1(a). Nanowire arrays were fabricated by electrochemically depositing Ni into the parallel, 2 μm long 12 nm diameter (sample No. 1) or 2.4 μm long and 16 nm diameter (sample No. 2) pores of the AAO films[2,3] using ac electrolysis. The fabrication of AAO films with varying pore diameters is a well established process.[1] The nickel wires are separated from the underlying, bulk aluminum substrate by a thin aluminum oxide barrier layer whose thickness can be varied reproducibly by varying the anodizing voltage during the template fabrication step. The barrier layer thickness, which forms the tunnel junctions was varied in the range 7 to 28 nm while keeping the pore diameter and pore density constant. (The pore density was controlled such that the mean interwire distance was 40 nm.) A scanning electron microscope (SEM) micrograph showing the top surface of a nickel-bearing AAO film and a typical measured diameter distribution function are also shown in Figs. 1(b), 1(c). The full-width at half height of the diameter distribution is approximately 16% of the mean diameter. The tips of the nickel wires at the end which is not next to the barrier layer were first exposed by partially chemically etching down the AAO matrix, then a silver electrode vapor deposited thereby shorting out the nickel wire array at that end.

Ordinary wire leads were then attached to the Al and Ag electrodes. The entire device then consists of an aluminum electrode, a thin aluminum oxide barrier layer, the array of individual nickel nanowires contained within an aluminum oxide matrix and a vapor-deposited silver electrode connecting all of the nickel nanowires approximately 2–2.4 μm above the tunneling barriers. Tunneling conductivity measurements were performed using standard modulation techniques.

A few typical tunneling spectra, $G(V)=dI/dV$, are shown in Fig. 2(a). The curves exhibit clear zero bias dips. The minimum deepens dramatically as the temperature is reduced below 5 K, however, the zero-bias conductivity does

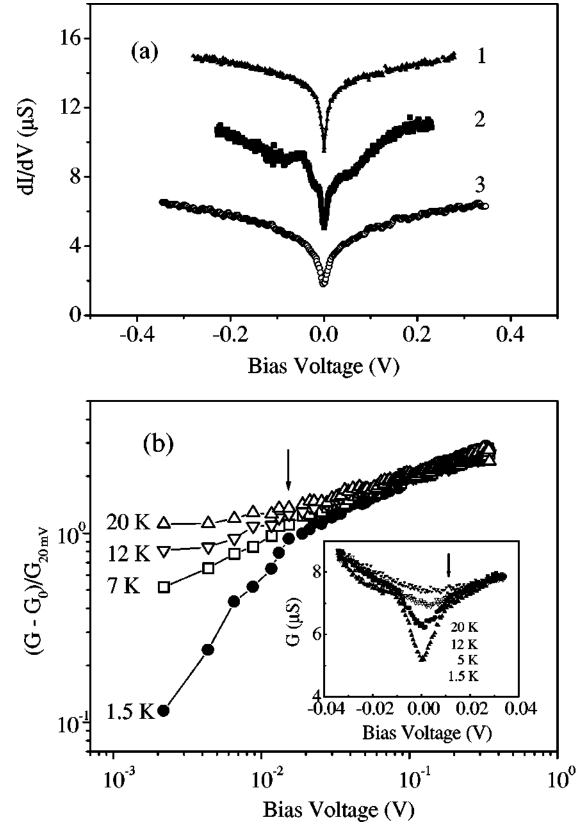

FIG. 2. (a) Examples of tunneling conductance G(V) spectra, curve 1: sample set No. 2, $T=3.5$ K, curves 2 and 3: two samples from the sample set No. 1, $T=1.5$ K. (b) Tunneling spectra corresponding to curve 3, the deviation from the square-root behavior is clearly observed at 1.5 K. Inset shows the temperature evolution of the zero bias dip corresponding to curve 2.

not extrapolate to zero at $T=0$. Figure 2(b) displays the conductivity measured at 1.5, 12, and 20 K as a log-log plot. Two conductivity regimes are observed at 1.5 K. For bias voltages above the voltage indicated by an arrow in Fig. 2(b) the tunneling conductance is more or less independent of temperature and dependent on voltage as $G\sim V^{\alpha}$ with $\alpha\sim 0.45$. Below that voltage the tunneling conductance is approximately a linear function of bias, i.e., $G_0\sim V$. At higher temperatures ($T>7$ K) the square-root voltage dependence is observed throughout the bias voltage range except at very low bias values where the temperature smearing of the Fermi function likely affects the conductivity.

The $G\sim V^{\alpha}$ [Fig. 2(b)] background can be attributed to electron-electron interactions in the disordered metal wires, in accord with Altshuler and Aronov.[13,14] This sort of behavior was previously reported for disordered Al films and doped semiconductors.[15,16] The effect originates in the nickel nanowire connected to the tunnel junction resulting in an additional contribution to the tunneling conductivity with approximately square-root voltage dependence of the form $G(eV)=G_0[1+(eV/\Delta)^{1/2}]$. The quantity Δ is related to the degree of disorder[15] and is known to depend on bulk resistivity as $\sim\rho^{-2}$.

The resistance of the individual nanowires which act as effective leads in intimate contact with the tunnel junctions is a key factor in determining whether CB is observable in our systems or not. We determined the individual nano-wire re-

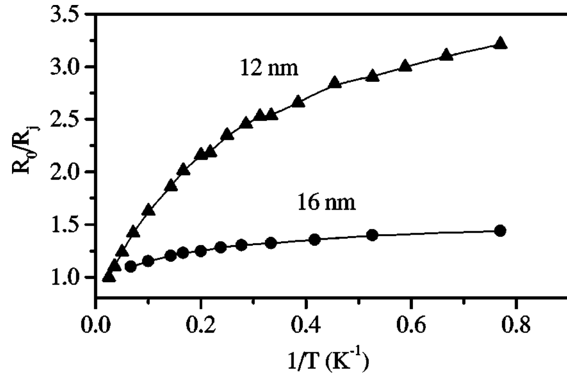

FIG. 3. Temperature dependence of the zero bias tunneling resistance for two sets of junction arrays, solid lines are guides to the eye.

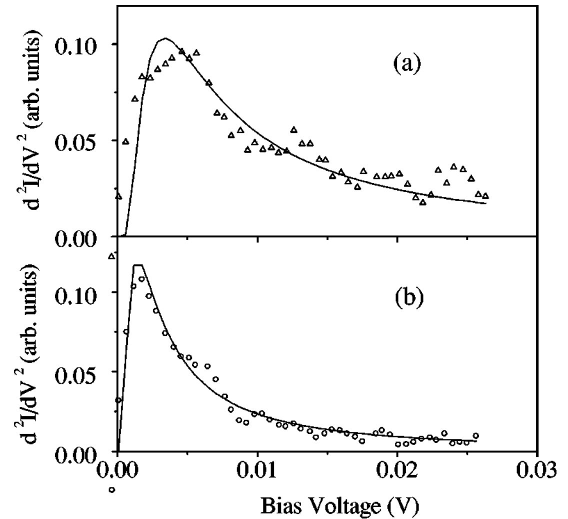

FIG. 4. The second derivatives of the tunneling current for (a) 12 nm diameter nanowires, (b) 16 nm diameter nanowires. Solid lines are fits to experimental data measured at 1.3 K.

sistance using scanning tunneling microscopy[17] yielding resistivity values $\sim(2.5-6.7)\times10^{-4}$ Ω cm at 300 K for various sets of samples. The quantity Δ was found to be approximately 0.25 eV at 1.5 K. The resistivity is approximately two orders of magnitude larger than for bulk polycrystalline Ni, suggesting a highly disordered metal. (Details of these measurements, carried out in nanowire arrays similar to those used in the present study, will be reported separately. The conductivity of nanowires also shows a square-root temperature dependence at low temperatures.[17])

Narrow zero-bias anomalies such as those shown in Fig. 2 are hallmarks of CB, however, for this interpretation to be invoked several conditions must be fulfilled. (1) For CB to be observed in single junctions, the values of junction and lead resistances, respectively, R_j and R_L, must each significantly exceed the resistance quantum $R_Q=h/2e^2$. The zero-bias dip is strongly suppressed when $R_L<R_Q=12.9$ kΩ, while for lead resistances greater than $\sim$ 40 kΩ, R_L is found to have almost no influence on the CB.[11] The total tunneling resistance of our junction array was measured to lie in the range of 100–500 kΩ. Each array consists of at most 10^{10} junctions, hence the total resistance of a single nanowire and its tunnel junction easily satisfies this condition. The lead resistance R_L which in our case is the resistance of a single cylindrical nanowire is 19–60 kΩ for the samples studied, as measured by STM. (2) The location of the high-resistance leads in immediate contact with the junction is also important for the observation of CB.[11]

Our arrays fulfill the above conditions suggesting *prima facie* that the observed conductivity-voltage behavior is due to Coulomb blockade. The inverse temperature dependence of the normalized zero-bias resistance is shown in Fig. 3 for the arrays based on 12 and 16 nm diameter nanowires. The substantially higher zero-bias resistance of the junctions fabricated from the higher-diameter wires [which have a lower metallic resistivity (8 vs 30 kΩ/μm)] and the location of the saturation point in the R_0/R_j vs $1/T$ curves for two sets of junction arrays, clearly demonstrate the effect of the lead resistance on CB. The effect of leads on CB in single junctions was considered by Nazarov.[18,19] Two different cases are described by him in where CB could be observed in single tunnel junctions. In the first case the inequalities $V>>\hbar C_0/R_0C_j^2e$ and $R_1\equiv C_jR_0/C_0>>R_Q$, must hold where C_0 and R_0 are the leads capacitance and resistance per unit length, respectively, and C_j is the junction capacitance. When these conditions are fulfilled the tunneling probability is completely suppressed in the bias voltage range $|V|<e/2C$. In a contrasting case $R_1<<R_Q$, while the total lead resistance R_0L remains larger than R_Q. In this event, the tunneling conductance is substantially but not completely suppressed and the Coulomb blockade is dominated by the leads. CB of the second type occurs in our tunnel junction arrays. The junction capacitance C_j can be roughly estimated as a flat plate capacitance between the bottom of each of the nanowires and the Al substrate $C_j\sim\epsilon\epsilon_0\pi a^2/d\sim3\times10^{-18}$ F, where a is the nanowire radius and d is the tunneling barrier thickness. The quantity R_0 was determined by direct measurement to be approximately 30 and 8 kΩ/μm at 4.2 K for the 12 nm and the 16 nm diameter samples, respectively.[17] This yields a value of the order of 1 kΩ for R_1. Hence, the leads play an important role.[18,19] Nazarov derived an analytical expression for the first derivative of the tunnel conductance as a function of bias as follows: $d^2I/dV^2R_0V_C=[4(V/V_C)^3]^{-1/2}\exp(-V_C/4V)$, where $V_C=e^3R_0/C_0\hbar$. This expression fits our measured results well (Fig. 4) using V_C values of 20 and 8.5 mV to fit the data extracted from the conductivity measurements performed on the 12 and 16 nm nanowire diameter samples, respectively. The values of C_0 determined from these V_C values are given in Table I. [The values obtained are in agreement with published estimates for $C_0\sim10^{-16}$ F/μm (Ref. 8)]. Accordingly, a substantial but incomplete suppression of tunneling is expected even at $T=0$ K when $V<V_C$.

The possible effect of stray capacitances must also be considered. At first glance it might seem remarkable that the capacitance C^* between the deposited Ag and the lower alu-

TABLE I. Nanowire junction parameters.

Sample	R_0 (Ω/μm)	V_C (mV)	C_0 (F/μm)	$C_{\rm eff}$ (F)
No. 1 (12 nm)	3×10^4	20	6×10^{-17}	3×10^{-17}
No. 2 (16 nm)	8×10^3	8.5	4×10^{-17}	8×10^{-17}

minum electrodes [Fig. 1(d)] does not mask the CB effects. A parallel plate capacitor with a surface area of 9 mm^2, an interelectrode spacing of 2 μm and filled with a material of dielectric constant 4 has a capacitance $C^* \sim 3\times10^{-11}$ F. Likewise one might worry about the interwire capacitance in the array. The effect of both of these sources of stray capacitance can be shown to contribute insignificantly to the effective capacitance of the device due to the length and poor conductivity of the nickel nanowires in contact with the tunnel junctions. These attributes effectively localize the electron tunneling event to a region near the junction thus decoupling it from the upper portions of the nanowire. As a result only the portion of the nanowire [of length δX_Q, say, Fig. 1(d)] whose resistance is $\sim R_Q$ Ref. 5 contributes to the effective capacitance that might influence the CB. This length of wire would contribute a capacitance $C_{\rm eff} = \delta X_Q C_0$, where C_0, is the capacitance per unit length (Table I) yielding $C_{\rm eff} = 3\times10^{-17}$ and 8×10^{-17} F for the two sets of samples studied. These values, together with the measured values of the resistivities per unit length (Table I), suggest that the nanowires will be decoupled from the tunnel junction at, approximately, 0.5 and 1.5 μm along their lengths for sample Nos. 1 and 2, respectively. (The overall lengths of the wires are 2 and 2.4 μm, respectively.) The fact that the effective junction capacitance is determined almost exclusively by the self-capacitance of this lower portion of the nanowire only is further implied by the observation that the zero-bias dip widths and hence the effective capacitances of tunnel junction devices fabricated with barrier thickness in the range of 7–28 nm were virtually identical.

The effect of the interwire capacitance $C_{\rm iw}$ [Fig. 1(d)] must also be considered. A simple estimate for $C_{\rm iw}$ is obtainable by noting that each nanowire is surrounded by six neighbors, a situation which might be modeled as a cylinder concentric with the nanowire positioned approximately at the location of the nearest neighbors, i.e., $C_{\rm iw} = 2\pi\delta X_Q \epsilon\epsilon_0/\ln(b/a)$, with $b=40$ nm and $a=6$ nm. This yields an interwire capacitance of the order of 3×10^{-16} F. However, the coupling between neghboring nanowires can be neglected due to the the smallness of the ratio $R_L/R_j \sim 10^{-4}$ which makes the voltage drop along the wires almost zero and hence the capacitive coupling negligible.

Single tunnel junction nanowire arrays were fabricated using a nonlithographic technique whereby Ni is deposited electrochemically in the pores of anodic aluminum oxide nanotemplates. The tunneling conductances of these arrays, studied as a function of bias voltage in the temperature range 1.3–40 K, displayed zero-bias anomalies whose temperature dependence strongly suggest Coulomb blockade as the origin. Stray capacitance was shown to affect the CB negligibly as a result of the high lead resistance which effectively decouples the tunnel junction. The results are in a good agreement with predictions of Nazarov[18] for the experimental regime where the device leads affect the details of the CB significantly.

We gratefully acknowledge the financial support provided by NSERC through both Research and Strategic grants. We thank K.K. Likharev, S. Kobayashi, and A.A. Tager for helpful discussions.

[1] D. Al-Mawlawi, C. Z. Liu, and M. Moskovits, J. Mater. Res. **9**, 1014 (1994).

[2] A. A. Tager, D. Routkevitch, J. Haruyama, D. Almawlawi, L. Ryan, M. Moskovits, and J.M. Xu, in *Future trends in Microelectronics*, Vol. 323 of NATO *Advanced Studies Institute*, Series E, edited by S. Luryi, J.M. Xu, and A. Zaslavsky (Kluwer Academic Publishers, Dordrecht, Boston, 1996), p. 171.

[3] D. Routkevitch, A. A. Tager, J. Haruyama, D. Almawlawi, M. Moskovits, and J. M. Xu, IEEE Trans. Electron Devices **43**, 1646 (1996).

[4] J. A. Switzer, C. J. Hung, B. E. Breyfogle M. G. Shumsky, R. van Leeuween, and T. D. Golden, Science **264**, 1578 (1994).

[5] D. V. Averin and K. K. Likharev, J. Low Temp. Phys. **59**, 347 (1985).

[6] H. R. Zeller and I. Giaever, Phys. Rev. **181**, 789 (1969).

[7] L. S. Kuzmin and K. K. Likharev, Jpn. J. Appl. Phys., Part 1 **26**, 1387 (1987); D. V. Averin and K. K. Likharev, in *Mesoscopic Phenomena in Solids*, edited by B. L. Altshuler, P. A. Lee, and R. A. Webb (Elsevier, Amsterdam, 1991), p. 173.

[8] P. Delsing, K. K. Likharev, L. S. Kuzmin, and T. Claeson, Phys. Rev. Lett. **63**, 1180 (1989).

[9] A. N. Cleland, J. M. Schmidt, and J. Clarke, Phys. Rev. B **45**, 2950 (1992).

[10] L. J. Geerligs, V. F. Anderegs, C. A. van der Jeugd, J. Romijn, and J. E. Mooij, Europhys. Lett. **10**, 79 (1989).

[11] Y. Shimazu, T. Yamagata, S. Ikehata, and S. Kobayashi, J. Phys. Soc. Jpn. **65**, 3123 (1996).

[12] K. P. Hirvi, J. P. Kauppien, A. N. Korotkov, M. A. Paalen, and J. P. Pekola, Appl. Phys. Lett. **67**, 2096 (1995).

[13] B. L. Altshuler and A. G. Aronov, Solid State Commun. **30**, 115 (1979).

[14] W. L. McMillan, Phys. Rev. B **24**, 2739 (1981).

[15] R. C. Dynes and J. P. Garno, Phys. Rev. Lett. **46**, 137 (1981).

[16] E. L. Wolf, in *Principles of Tunneling Spectroscopy* (Oxford University Press, New York, 1985), and reference therein.

[17] D.N. Davydov, A. Osika, D. Routkevitch, C. Cornu, B. W. Statt, M. Moskovits, and J.M. Xu (unpublished).

[18] Yu. V. Nazarov, Sov. Phys. JETP **68**, 561 (1989); JETP Lett. **49**, 126 (1989).

[19] G. L. Ingold and Yu.V. Nazarov, in *Single Charge Tunneling* (Plenum, New York, 1992).